

Parallel Composition of Templates for Tail-Energized Planar Hopping

Avik De*

Daniel E. Koditschek*

Abstract— We have built a 4DOF tailed monopod that hops along a boom permitting free sagittal plane motion. This underactuated platform is powered by a hip motor that adjusts leg touchdown angle in flight and balance in stance, along with a tail motor that adjusts body shape in flight and drives energy into the passive leg shank spring during stance. The motor control signals arise from the application in parallel of four simple, completely decoupled 1DOF feedback laws that provably stabilize in isolation four corresponding 1DOF abstract reference plants. Each of these abstract 1DOF closed loop dynamics represents some simple but crucial specific component of the locomotion task at hand. We present a partial proof of correctness for this parallel composition of “template” reference systems along with data from the physical platform suggesting these templates are “anchored” as evidenced by the correspondence of their characteristic motions with a suitably transformed image of traces from the physical platform.

I. INTRODUCTION

The control of power-autonomous, dynamic legged robots that have a high number of degrees of freedom (DOF) is made difficult by a number of factors including (a) under-actuation necessitated by power-density constraints, (b) the existence of significant inertial coupling and Coriolis forces that are hard or impossible to cancel, (c) variable ground affordance, (d) often hard-to-measure and necessarily rapid hybrid transitions. In the face of these challenges, some popular methods of controller design, such as hybrid zero dynamics [1]—which are “exact” in their domain of applicability but require extremely accurate qualitative and quantitative models—may be challenging to implement in unstructured environments or on imperfectly characterized machines. Similarly, methods depending on local linearizations of the typically (highly) nonlinear dynamics found in dynamically dexterous locomotion and manipulation systems [2], [3] typically suffer from small basins of attraction [4] and (to our knowledge) high sensitivity to parameters.¹

Observation (a) suggests that modularity of operation (i.e., wherein different combinations of actuators are used to effect distinctly different dynamical goals at different stages within the task cycle) will be a hallmark of practical locomotion platforms. Observations (b) and (c) imply that simpler, less exact but potentially more robust representations of the principal dynamical effects likely to prevail across

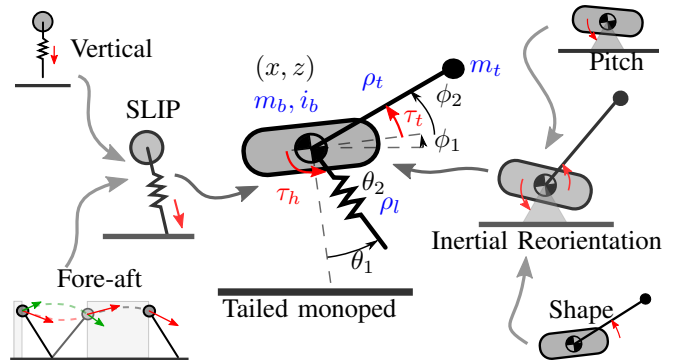


Fig. 1. Control of a hopping behavior expressed as a hierarchical composition of closed-loop templates. Notionally, the grey arrows represent directed template→anchor relations. **Center:** A model of the tailed monopod physical platform on which we implement tail-energized planar hopping, labeled with configuration variables (black), actuators (red), and model parameters (blue).

a wide range of substrates may offer a tractable means of working with rather than fighting against, or learning exactly the highly varied dynamical details. Observation (d) implies that higher authority sensorimotor control activity ought to target continuous phases of the locomotion cycle, leaving the transition event interventions to more passive and mechanical sources of regulation [6]. In sum, these observations motivate the search for modular, reduced order representations of locomotion task constituents that are specialized to couple selected actuation affordances to particular DOFs at particular phases of the locomotion cycle. The value of such component task representatives remains hostage to the availability of methods for composing them in a stable manner.

This report introduces a novel locomotion platform, the Penn Jerboa, Fig. 2, to put a slowly maturing formalism for the composition of such modules to a practical test. We adopt the template-anchor² framework [9] to represent this machine’s 4DOF steady sagittal plane running as the hierarchical composition of the low DOF constituents depicted in Fig. 1. At the leaves of this hierarchy tree, we introduce four different 1DOF templates that emerge from the decades old bioinspired running literature [3], [10],

*Electrical and Systems Engineering, University of Pennsylvania, Philadelphia, PA, USA. {avik,kod}@seas.upenn.edu.

This work was supported in part by the ARL/GDRS RCTA project, Coop. Agreement #W911NF-1020016 and in part by NSF grant #1028237.

¹In some robotics settings these disadvantages of the exact or local linearized control paradigm can be effectively remedied by recourse to parameter adaptation [5], but in our experience, such methods are too “laggy” to work in this hybrid dynamics domain with its intrinsically abrupt and rapidly switching characteristics.

²The template-anchor relation as exemplified in various physical [4], [7] and numerical [8] studies associates a pair of smooth vector fields, f^T, f^A on a pair of smooth spaces, $\mathcal{T} \subset \mathcal{A}$ via the condition that \mathcal{T} is an attracting invariant submanifold of the anchor field, f^A , whose restriction dynamics is conjugate to that of the template field, $f^T \sim f^A|_{\mathcal{T}}$ (where \sim denotes equivalence up to smooth change of coordinates). In this paper, we are dealing with hybrid fields and flows for which the extended definition and its verification is a bit more intricate. Thus exceeding the scope and length constraints of the present paper, we will treat the hybrid template-anchor relation as an intuitive notion here.

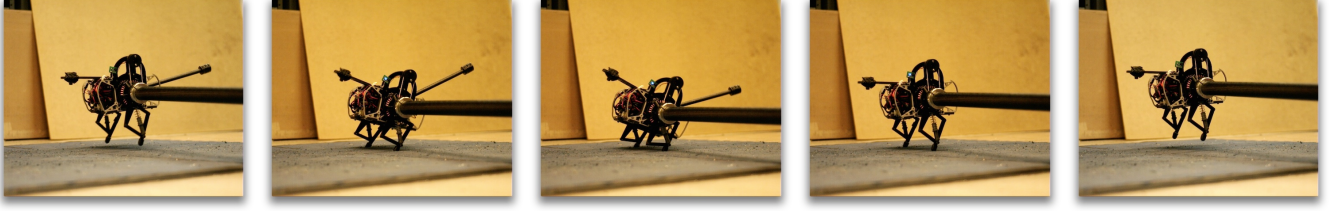


Fig. 2. Snapshots from apex to apex of tail-energized planar hopping (§V) implemented on a new robot platform—the Penn Jerboa (§VI).

joined by a new arrival from recent work on bioinspired tails [11], [12]. We apply the four decoupled 1DOF control laws associated with these isolated “leaf” templates directly to the (highly dynamically coupled) physical platform and demonstrate empirically steady sagittal plane running (on a circular boom) whose body motions reveal, when viewed in the appropriate coordinates, Fig. 7, striking similarity to the corresponding isolated 1DOF constituents. We show (up to a still unproven technical conjecture) that the appropriate two pairs of these four 1DOF leaf templates are formally anchored by the two “interior” 2DOF templates depicted in Fig. 1, in the sense that the 1DOF systems define attracting invariant submanifolds of the 2DOF systems that exhibit conjugate restriction dynamics. We conjecture, as well, that the two interior nodes (the 2DOF templates) of the figure are in turn formally anchored by a physically realistic dynamical model of the closed loop Penn Jerboa in the sagittal plane. The data of Fig. 7 support this hypothesis, but we have not yet succeeded in completing the proof beyond the embedding and invariance properties.

Notwithstanding the specifics of our compositional approach to its control, we believe that the new physical platform is itself of independent interest by virtue of its added appendage (the “tail”), opening up a multiplicity of diverse uses for both of its two revolute actuators. Note again, however, this diversity of uses cannot be achieved without some recourse to behavioral modularity. In that light, we are particularly attracted by these simple low-DOF template controllers. In our experience, such constructions have the hope of succeeding in unstructured outdoor settings, since they build on the relatively robust template dynamics.

A. Relation to Prior Literature

This “compositional” method of controller synthesis was pioneered empirically by Raibert [13] for planar and 3D hopping machines, and we develop our planar hopping behavior by building up from those ideas. Our physical platform (Fig. 1 center) forgoes Raibert’s prismatic shank actuator, and instead places that actuator in an inertial appendage. This motivates us to explore how tails can be “recycled” from their transitional agility duties [11], [12], now repurposed to substitute for Raibert’s shank actuator and play the role of steady-state running energizer in the sagittal plane. Apart from their use in transitional maneuvers (inertial control in free-falling lizards [14] and robots [11], [12] or in turning lizards [15] and robots [16]) it has recently been discovered that kangaroos do positive work with their tails

TABLE I
LIST OF SYMBOLS

$i \in \mathbb{Z}_2$	Hybrid mode, where 1 is stance, 2 is flight
\mathcal{D}_i^*	Domain for template \star in mode i
$f_i^* : \mathcal{D}_i^* \rightarrow T\mathcal{D}_i^*$	Vector field in mode i
$r_i^* : \partial\mathcal{D}_i^* \rightarrow \mathcal{D}_{i+1}^*$	Reset map from mode i to $i + 1$
$F_i^* : \mathcal{D}_i^* \rightarrow \partial\mathcal{D}_i^*$	Mode i flow evaluated at the next transition
$F^* = F_2^* \circ F_1^*$	Return map at touchdown (TD) event
$p_i^*(x, u)$	Plant to which we apply $u = g_i(x)$ to get f_i^*
$I_d \in \mathbb{R}^{d \times d}$	Identity matrix of size d
$J = \begin{bmatrix} 0 & -1 \\ 1 & 0 \end{bmatrix}$	Planar skew-symmetric matrix
$e_i \in \mathbb{R}^d$	i^{th} standard basis vector
$R : S^1 \rightarrow \text{SO}(2)$	Map from angle to rotation matrix
$Tx = (x, \dot{x})$	Tangent vector associated with x
$D_x y$	Jacobian matrix $\partial y_i / \partial x_j$
$\kappa \in \mathbb{R}_+$	SLIP radial velocity gain (§III-B.2)
$h_\kappa \in \mathbb{R} \rightarrow \mathbb{R}_+$	Map from radial TD velocity to κ (§III-A.1)
$\gamma : \mathbb{R} \rightarrow S^1$	Fore-aft model stance sweep angle (§III-B.2)
$\beta : \mathbb{R} \rightarrow S^1$	Raibert touchdown angle function (8)
$h_w : \mathbb{R}^2 \rightarrow \mathbb{R}^2$	Cartesian to Polar TD velocity (§III-C.2)

TABLE II
TEMPLATE CONTROLLERS

Tail energy pump	$g_1^v(x) = k_t \cos(\angle x)$	(3)
Raibert stepping [13]	$g_2^{\text{fa}}(\dot{x}) = \beta^*(\dot{x}) + k_p(\dot{x} - \dot{x}^*)$	(8)
Raibert pitch correction [13]	$g_1^p(a_1, \dot{a}_1) = -k_g k a_1 - k_g \dot{a}_1$	(15)
Shape reorientation [12]	$g_2^{\text{sh}}(a_2, \dot{a}_2) = -k_g k a_2 - k_g \dot{a}_2$	(15)

in a quasistatic pentapedal gait [17]. In our implementation, the tail contributes the reorientation function in flight, and the energetic “pump” function in stance (albeit in a dynamic fashion). We are not aware of prior robotic locomotion work wherein a tail is used to help power the stance phase.

B. Contributions of the Paper

This paper contributes both to the theory and practice of dynamical legged locomotion.

The principal theoretical contributions are: (i) a new (slightly simplified) further abstraction (§III-C) of the long-standing SLIP running model [3] as a formal cross-product of previously proposed vertical [18] and fore-aft [19] templates; (ii) a stability proof (modulo a restrictive assumption 3) of

the parallel composition³ of Raibert’s [13] stepping controller (8) with our new energy pump (3) in Proposition 5; and (iii) a proof of local stability in the inertial reorientation model (14) of the parallel composition (15) of Raibert’s [13] pitch stabilizer and the tail reorientation controller [12] in Proposition 6.

The empirical contributions of the paper are: (i) design and implementation of a working tailed biped platform, the Penn Jerboa [20] (Fig. 2); (ii) physical demonstration of the (provably correct–Proposition 1) oscillatory spring-energization scheme for vertical hopping; and (iii) experimental evidence supporting the hypothesis that our final parallel composition of the four isolated controllers does indeed anchor the corresponding templates in the Jerboa body (Fig. 7).

II. PRELIMINARIES: ORGANIZATION AND NOTATION

Table I contains a list of important symbols in this paper, including a set of symbols for describing hybrid dynamical systems. We adopt the modeling paradigm from Definition 1 in [21], representing a hybrid dynamical system by the tuple (\mathcal{D}, f, r) as defined in Table I. We only consider two hybrid modes in this paper: ballistic flight, and a stance phase arising from a sticking contact at the “toe”.

Superscripts on each of these symbols denote the *hybrid template* that it is a part of, e.g. \star^v for controlled vertical hopping (§III-A). The layout of the paper roughly reflects the template-anchor hierarchy depicted in Fig. 1. Namely, there are two intermediate 2DOF templates—the SLIP, s , and the inertial reorientation, a —that comprise the tailed monopod, $tm = \{s, a\}$. They, in turn, are comprised of the vertical, v , and fore-aft, fa , 1DOF templates, $s = \{v, fa\}$, and respectively, the shape, sh , and pitch, p , 1DOF templates, $a = \{sh, p\}$. We endow the 1DOF templates at the lowest level with an exemplar plant, with respect to which we will develop controllers for the four template plants, in isolation.

Sections III-IV present the 2DOF s, a templates that are directly anchored in the robot body (§V), and within them contain descriptions of the subtemplates (e.g. §III-A, III-B)—as simple exemplar 1DOF anchoring bodies and corresponding control laws—that comprise in isolation the constituent desired limiting behaviors that we seek to embody simultaneously in our physical system. Each of the template controllers in this suite is necessarily simple by dint of its origin as a feedback law for a highly abstract 1DOF task exemplar. We hypothesize that this combination of algorithmic simplicity and task specialization may lend robustness in the empirical setting since control policies are not sensitive to, and certainly avoid cancellation of, forces arising from dynamical coupling in the anchoring body.

We emphasize that these coupling-naïve feedback laws (summarized in Table II) are simply “played back” (modulo scaling) in the 6DOF body (§V) with all its complicated true dynamical coupling. We show formally through various

³By this term we mean the application to the (coupled) plant $p^s(x, u)$ (§III-C) of a decoupled control law, $u = g^v(x_1) \times g^{fa}(x_2)$, taken directly from (3), (8), respectively.

propositions in this paper that nevertheless the stability of the templates and subtemplates persists through composition for the distal segments of the tree (Fig. 1)—SLIP as a composition of vertical hopping and fore-aft speed control, and attitude stabilization as a composition of inertial reorientation and Raibert’s pitch control. We provide some preliminary suggestions about the composition of SLIP (s) with attitude (a) compartments (center of Fig. 1), but a full analysis is left to future work. However, we offer empirical data in §VI showing how this idea has resulted in promising qualitative behavior on the Jerboa robot (Fig. 7, video attachment).

Note: Due to space constraints, we have moved the proofs as well as additional experimental results to a companion technical report [20].

III. THE (2DOF) SLIP TEMPLATE

A. Controlled Vertical Hopping (1DOF)

For a successful hopping behavior, energy must be periodically injected into the robot body to compensate for losses. We simplify the analysis here to a 1DOF vertically-constrained point-mass which can alternate between stance phase (during which the actuator has affordance) and a ballistic (passive) flight phase. It has been shown in the past empirically [13] and analytically [22] that an impulse at the bottom of stance can produce a stable limit cycle, in the presence of a spring for energy storage. In this paper, we consider a different strategy of an actuator forcing the damped spring by applying forces in a phase-locked manner. This choice of input representative is made with an eye toward using a tail actuator exerting inertial reaction forces on the spring (this model is formally instantiated §V). Intuitively, this can be thought of as negative damping [18] (effectively cancelling losses by physical damping).

Throughout this paper, we make the following assumption inspired by [13]:

Assumption 1 (Stance duration). *The duration of stance, T_s , is approximately constant.*

This essentially asserts that the damping losses or actuator forces are relatively small compared to the spring-mass dynamics (in their effect on the liftoff condition).

We build upon the “linear spring” analysis in [22] for our vertical hopping exemplar body and closed-loop template. For a spring-mass-damper system with spring deflection χ , damping coefficient $\bar{\beta}$ and natural frequency ω

$$\ddot{\chi} + 2\omega\bar{\beta}\dot{\chi} + \omega^2\chi = \tau. \quad (1)$$

With the change of coordinates $x_1 := \chi$, $x_2 := \dot{\chi}/\omega$,

$$\dot{x} = p_1^v(x, \tau) := -\omega Jx + e_2^T(-2\bar{\beta}\omega x_2 + \tau/\omega), \quad (2)$$

and the hybrid reset events occur at $x_1 = 0$ (corresponding physically to the touchdown and liftoff events at $\chi = 0$).

1) *Oscillatory Spring Energization:* We choose the physically motivated control strategy

$$\tau := \frac{k_t x_2}{\|x\| + \varepsilon} \approx k_t \cos \angle x, \quad (3)$$

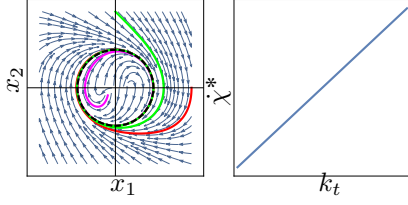


Fig. 3. **Left:** The vector field and an execution of (4), showing a stable limit cycle. **Right:** The vertical “energy” is easy to tune with k_t .

where $\varepsilon > 0$ is a small saturation constant. It is clear in this form that the input is a fed-back version of the “phase” only. We obtain the closed-loop stance dynamics

$$\dot{x} = f_1^v(x) := -\omega Jx + \left(-2\bar{\beta}\omega + \frac{k_t}{\omega(\|x\| + \varepsilon)}\right) x_2 e_2. \quad (4)$$

Proposition 1 (Oscillatory energization stability). *The vertical hopping template (4) has a unique attracting periodic orbit.*

Proof. Included in [20]. \square

As a corollary to Proposition 1, we know F_1^v (the vertical stance map, cf. [20]) has an asymptotically stable fixed point, $\dot{\chi}^*$, and $-1 < DF_1^v|_{\dot{\chi}^*} < 1$.

Ballistic flight simply reverses the velocity,

$$F_2^v(\dot{\chi}) := -\dot{\chi}. \quad (5)$$

Note that by symmetry (f_1^v , and consequently F_1^v are odd), $F_1^v \circ F_1^v = F_2^v \circ F_1^v \circ F_2^v \circ F_1^v$, i.e. the stability properties of the hybrid system are the same as that of the stance map as analyzed in Proposition 1. Define

$$\kappa = h_\kappa(\dot{\chi}) := \frac{-F_1^v(\dot{\chi})}{\dot{\chi}}, \quad (6)$$

the effective coefficient of restitution through stance, or the so-called “velocity gain” during SLIP stance [19]. Note that there is a unique fixed point, $\kappa^* = 1$, in these coordinates, which is necessary and sufficient for the smooth invertibility of h_κ , as can be seen by direct computation of its derivative.

Conjugating the touchdown velocity return map via this diffeomorphism, we can define a return map for κ , F^v ,

$$F^v(\kappa) := h_\kappa \circ F_2^v \circ F_1^v \circ h_\kappa^{-1}(\kappa) = h_\kappa(\kappa h_\kappa^{-1}(\kappa)). \quad (7)$$

Proposition 2 (Vertical stability). *The velocity gain return map, F^v , has an asymptotically stable fixed point, $\kappa^* := 1$, and $DF^v|_{\kappa=1} = -DF_1^v|_{\dot{\chi}^*}$.*

Proof. Included in [20]. \square

B. Controlled Fore-Aft Speed (1DOF)

Running and walking systems of a large variety from the sagittal or frontal plane resemble inverted pendula during stance [3], usually controlled by stepping strategies. It has been shown that a fixed touchdown angle can admit a reasonable basin of stability around an emergent attracting steady-state velocity in SLIP [23]. The capture point [24] and zero moment point [25] methods use a quasistatic heuristic

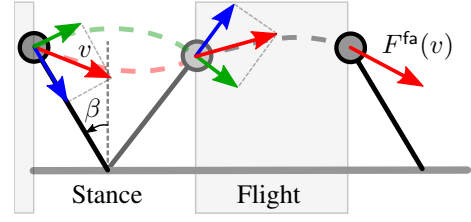


Fig. 4. A simple model for the 1DOF fore-aft dynamics in SLIP, closely related to BHop [19].

which is related to these ideas, but are not explicitly designed to servo to desired nonzero speeds. We attempt here to place the empirical success of [13] in the context of a model where its stability properties can be analyzed.

1) *The Raibert Stepping Controller:* In his classical empirical study, Raibert [13] inspired decades of subsequent experimentation and analysis by offering the following observations⁴ about the pendular stance phase in his running machine travelling at forward speed, \dot{x} , and stepping with a touchdown angle $\beta(\dot{x})$ (as in Fig. 4):

Assumption 2 (Raibert observations). (i) *For each speed, \dot{x} , there is a neutral⁵ touchdown angle, $\beta^*(\dot{x})$ (ii) this neutral angle is monotonic with speed, $D_{\dot{x}}\beta^* > 0$, and (iii) deviations from touchdown angle cause negative acceleration, i.e. $D_{\beta}(\dot{x}^+ - \dot{x})|_{\beta=\beta^*} < 0$.*

Proposition 3 (Raibert stepping controller). *Under assumptions 2(i-iii), the Raibert stepping controller,*

$$\beta : \dot{x} \mapsto \beta^*(\dot{x}) + k_p(\dot{x} - \dot{x}^*) \quad (8)$$

stabilizes the forward speed to \dot{x}^ .*

Proof. Included in [20]. \square

2) *Modified BHop as a Fore-Aft Model:* Building on existing SLIP literature [26], we make the following assumptions about pendular stance:

Assumption 3 (Pendular stance). *During stance, (i) the effects of gravity are negligible⁶ compared to spring potential / damping forces, (ii) radial deflections are negligible, (iii) time of stance is constant, and (iv) the angle swept by the leg admits a small-angle approximation.*

Schwind [26] approximated that angular momentum about the toe is constant during stance, but we simplify further with the second assumption, and conclude that the angular velocity is roughly constant during stance. We adopt the third approximation from Raibert [13], and the last approximation is made for the ensuing analytical simplifications in §V-B, but we find empirically (§VI) that it is not critical in practice.

⁴These conditions are not a direct result of SLIP’s nonlinear dynamics, but are applicable to regime of interest.

⁵In this context, “neutral” means $\dot{x}^+ = \dot{x}$, where \dot{x}^+ refers to the fore-aft speed at the subsequent touchdown event.

⁶We suspect that the less restrictive Geyer approximation [27] is sufficient, but leave this generalization to future work.

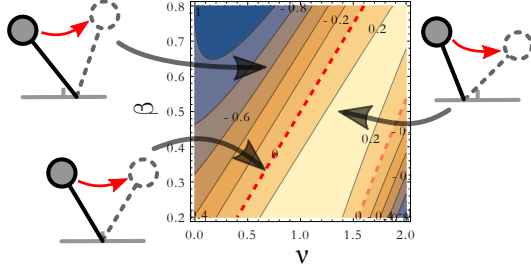


Fig. 5. A contour plot of the fore-aft acceleration $\dot{x}^+ - \dot{x}$ produced by the MBHop model for a range of fore-aft speed \dot{x} and touchdown angle β . This plot depicts that (in a range around the neutral angle), this model captures all the conditions of assumption 2.

These assumptions lead directly to the construction of the following return map acting on touchdown velocity in Cartesian coordinates (cf. Fig. 4). Then,

$$\begin{aligned} F^s(v, \kappa) &= \begin{bmatrix} 1 & -1 \end{bmatrix} R(-\gamma + \beta) \begin{bmatrix} 1 & -\kappa \end{bmatrix} R(-\beta)v \\ &= R(\gamma - \beta) \begin{bmatrix} 1 & \kappa \end{bmatrix} R(-\beta)v, \end{aligned} \quad (9)$$

where κ (explicitly, the interaction from the radial component of SLIP) is taken to be a fixed parameter at this stage, $\gamma(v_1) \approx \frac{v_1 T_s}{\rho_l}$ is the angle swept by the leg over the course of stance and $\beta(v_1)$ is the leg touchdown angle (§III-B.1). This model is only a slight modification⁷ of BHop [19].

This analytically tractable model (i) allows us to “separate” the radial dynamics (encapsulated in κ) from the contributions of the fore-aft model itself, (ii) captures the exchange of vertical and horizontal energy through stepping, and (iii) matches the empirically observed Raibert conditions (Fig. 5) as well as empirical data (Fig. 7), suggesting it is physically applicable and not just an analytical convenience.

For now we restrict our attention to $\kappa = 1$, and generalize to include the radial dynamics in §III. With this restriction,

$$F^{\text{fa}}(v) := F^s(v, 1) = R(\gamma - 2\beta)v, \quad (10)$$

While we choose to parameterize the return map as a function of $v \in \mathbb{R}^2$, it is really a 1D map:

Proposition 4 (Fore-aft stability). *MBHop with the Raibert controller presents a stable touchdown return map.*

Proof. Included in [20]. \square

C. SLIP as a Parallel Composition

In order to anchor our 1DOF templates in the classical SLIP model (2DOF point mass with 2DOF springy leg), we simply “play back” our devised control schemes (Sections III-A and III-B). In the following subsections, we check that the closed-loop executions in the higher-DOF body still resemble a cross-product of our template behaviors. For instance, prior literature has observed a decomposition of SLIP dynamics into radial and tangential components, but to

⁷Specifically, the similarities are apparent between (9) and (19) of [19]. The slightly discrepancy should be attributed to our insistence on using the physical touchdown and sweep angles β and γ in the model, whereas the abstract parameter θ in [19] results in a more succinct form.

our knowledge there is no complete account of the stability of the parallelly composed (closed-loop) templates in these components.

1) *Hybrid Dynamical Model of SLIP:* We will construct our template plant model from [26]: a bead of mass 1 at (Cartesian) coordinates $(x^s, z^s) \in \mathbb{R}^2$, with a springy (Hooke’s law spring constant k_s) massless leg of length⁸ $\theta_2^s \in \mathbb{R}_+$ (where \mathbb{R}_+ is restricted to *strictly* positive reals, and is open) and rest length ρ_l , at an angle of $\theta_1^s \in S^1$ from vertical. Let $\mathbf{q}^s := (\theta_1^s, \theta_2^s, x^s, z^s)$. Using assumption 3(iv) as a convenience (though that assumption is not required for this formulation), the touchdown and lift-off conditions can be specified in terms of the zeros of $\mathbf{a}^s := z^s - \rho_l$.

Define $\mathcal{Q}_i^s := S^1 \times \mathbb{R}_+ \times \mathbb{R} \times \mathcal{I}_i$, where $\mathbb{R} = \mathcal{I}_1 \sqcup \mathcal{I}_2 := (-\infty, \rho_l] \sqcup (\rho_l, \infty)$. Then, $\mathcal{D}_i^s := T\mathcal{Q}_i^s$, and

$$f_1^s(\mathbf{q}^s, \dot{\mathbf{q}}^s) := \left(\dot{\mathbf{q}}^s, \begin{bmatrix} -\frac{2\theta_1^s \theta_2^s}{\theta_2^{s2}} \\ \theta_2^s \theta_1^{s2} + k_s(\rho_l - \theta_2^s) \end{bmatrix} \right), \quad (11)$$

$$f_2^s(\mathbf{q}^s, \dot{\mathbf{q}}^s) := \left(\dot{\mathbf{q}}^s, \begin{bmatrix} 0 \\ -g \end{bmatrix} \right), \quad (12)$$

where the unspecified components are (i) the mass-center dynamics which are constrained by $\begin{bmatrix} x^s \\ z^s \end{bmatrix} = \theta_2^s \begin{bmatrix} -\sin \theta_1^s \\ \cos \theta_1^s \end{bmatrix}$ in (11), and (ii) the degenerate massless leg dynamics in (12).

We explicitly write the guard set and reset map in [20].

2) *Anchoring the 1DOF Templates:* Consequent upon the above model—where each hybrid mode is dynamically 2DOF—SLIP is a 4D dynamical system (one parameterization being (x, z, v) , where $v \in \mathbb{R}^2$ is the touchdown velocity, and $(x, z) \in \mathbb{R}^2$ is the Cartesian location of the point mass at touchdown). The efficacy of our 2D return map analysis is established by arguments similar to those of [29]: the Poincare section $z^{\text{TD}} = \rho_l \cos \beta(v)$ eliminates one dimension, and the equivariance of the dynamics with x eliminates another.

We first observe that our MBHop model of §III-B.2 still represents the pendular stance correctly under assumption 3. However, κ is not a fixed parameter, but evolves according to dynamics similar to F^v in Proposition 2. From (8) and (9), the embedded ($\kappa = 1, v = v^*$) submanifold is invariant. We show in Proposition 5 that it is also attracting.

Let us define $h_w : \mathbb{R}^2 \rightarrow \mathbb{R}^2$ as

$$w = h_w(v) := R(-\beta(v))v. \quad (13)$$

This mapping is a local diffeomorphism (cf. [20]), and the vector w gives a tangential/radial decomposition of v (i.e. polar with respect to the leg angle).

Additionally, using (6), we can “recover” the κ -dynamics in the coupled system: $\kappa = h_\kappa(w_2)$. We prefer the redundant (v, κ) parameterization because of analytical tractability.

Proposition 5 (Stability of SLIP as a composition). *For (i) stable vertical hopping with $-1 + \varepsilon_r < -DF_1^v|_* < 1 - \varepsilon_r$, (ii) sufficiently⁹ small k_p in the Raibert controller, parallel composition of the radial and fore-aft templates results in a locally stable 2D return map, F^s .*

⁸We use θ for leg “joints” to be consistent with [28].

⁹Formally, this means that k_p can be chosen as a function of ε_r .

A. Modeling for Planar Hopping

Raibert’s planar hopper [13] empirically demonstrated stable hopping using a rigid body with a springy leg, and in this paper we pursue the same idea, but instantiate vertical hopping by coupling the 1-DOF leg-spring excitation controller (physically acting through the tail). In flight, the tail actuator grants us a new affordance that we only¹⁰ use here to regulate the added “shape” DOF. Our physical model is shown in Fig. 1 (center). The system has a single massless leg with joints $\theta = (\theta_1, \theta_2) \in S^1 \times \mathbb{R}_+$, a rigid body $(x, z, \phi_1) \in \text{SE}(2)$, and a point-mass tail with revolute DOF ϕ_2 , such that the full configuration is $\mathbf{q} := (\theta_1, \theta_2, x, z, \phi_1, \phi_2) \in \mathcal{Q}$. We make the following design-time assumptions:

Assumption 4. (i) *Leg/tail axes of rotation are coincident at the “hip,”* (ii) *tail mass is small, i.e. $m_t \ll m_b$,* (iii) *center of mass (configuration-independent by the previous assumption) coincides with the hip, and (iv) body, tail have high inertia, i.e. $i_b, i_t \rightarrow \infty$.*¹¹

We derive the equations of motion in [20].

B. “Physical” Decoupling and Anchoring

With the highly restrictive assumption 4 (allowing for infinite tail inertia), the tail motion is essentially negligible. Under these conditions, we show the emergence of the beginnings of a classical anchoring relation [9], via a natural (weak) decoupling of the 6DOF dynamics into “point-mass” and attitude compartments. A more general analysis that is more physically relevant is forthcoming in future work.

Proposition 7 (Flow-invariant submanifold). *Under assumption 4, in each hybrid mode, (i) the submanifold $\mathcal{U} = \{T\mathbf{q} \in T\mathcal{Q} : T\phi_1 = T\phi_2 = 0\}$ is invariant under the action of the flow generated by f_i^{tm} , and (ii) in each hybrid mode, the closed-loop flow restricted to \mathcal{U} , $T\mathbf{q} = f_i^{\text{tm}}(T\mathbf{q}|_{\mathcal{U}})$ is a cross-product of the template vector fields,*

$$f_i^{\text{tm}} = f_i^s \circ \pi_s \times f_i^a \circ \pi_a, \quad (17)$$

where π_s and π_a represent projections to the SLIP and attitude components of \mathbf{q} respectively.

Proof. Included in [20]. \square

Additionally, the invariant submanifold in the flow leads to an invariant submanifold in the hybrid execution:

Proposition 8 (Return map-invariant submanifold). *The set \mathcal{U} is invariant under the return map $F^{\text{tm}}(T\mathbf{q}|_{\mathcal{U}})$, and restricted to \mathcal{U} , $F^{\text{tm}} = F^s \circ \pi_s \times F^a \circ \pi_a$.*

Proof. Included in [20]. \square

We leave to future work a proof that \mathcal{U} is attracting, which is a requirement for demonstration of anchoring [9].

¹⁰We avoid a detailed discussion here, but a revolute tail avoids the morphological specialization of a dedicated prismatic actuator and can be repurposed for other uses such as static standing, reorienting the body in free fall [12], directing reaction forces through ground contact for leaping when used as another “leg” [31], etc.

¹¹Even though the dynamic task here is quite different from free-fall, in the language of [12] this is saying that the tail should be light but *effective*.

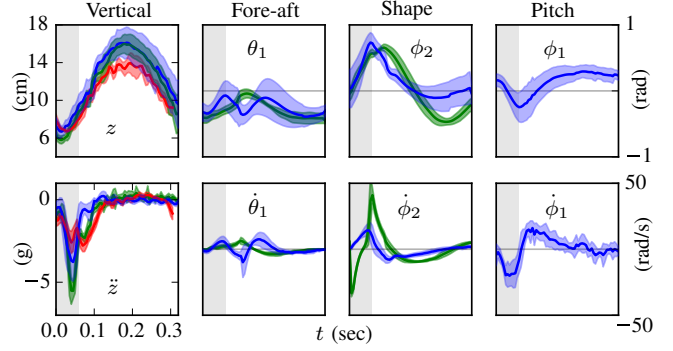


Fig. 7. A single stride (stance with shaded background followed by flight), where each column corresponds to some representative time series from each of the four 1DOF templates from §III-IV, and the traces (mean and standard deviation) correspond to different “bodies” realized by variably constraining the robot—**red**: tailed vertical hopper (i.e. (θ_1, x, ϕ_1) locked), **green**: tailed point-mass hopper (i.e. ϕ_1 locked), **blue**: tailed planar hopper (all free)—in which these templates are being anchored.

VI. EXPERIMENTAL RESULTS

We perform the experiments on the Penn Jerboa: a new tailed bipedal robot platform (Fig. 2) with a pair of compliant hip-actuated legs (in parallel for sagittal plane behaviors), and a 2DOF revolute point-mass tail [12] driven differentially by two motors through a five-bar mechanism (locked in the sagittal plane for the behaviors in this paper). We include a detailed design report as well as additional experimental results including the effect of varying tail mass, and empirical validation of our pitch/shape decomposition of §IV in [20].

By physically constraining some of the DOFs, we test our hierarchical composition (Fig. 1) at as many “nodes” of the composition tree as possible. Note that it is infeasible to isolate the fore-aft or the closed-loop pitch correction templates in a physical setting. The results are summarized in Fig. 7. Five strides are averaged within each category, and aligned with ground truth knowledge of the touchdown event. We observe that

- i) there is a vertical limit cycle that retains its rough profile and magnitude through three anchoring bodies,
- ii) the hip angle roughly satisfies $\ddot{\theta}_1 = 0$ in stance and the stance duration is roughly constant (corroborating assumptions 3.ii-iii, and our MBHop model (9),
- iii) the shape coordinate is destabilized in stance and stabilized in flight, and the pitch-deflections are small in magnitude over the stride, and in agreement with (16).

Qualitatively, the “tailed point-mass hopper” configuration attained stable forward hopping at controlled speeds upwards of 20 strides, only limited by space. The fully unlocked system has so far hopped for about 10 strides at multiple instances before failing due to accumulated error causing large deviations from the limit cycle. We believe the prime reason for this is that the CoM is significantly aft of the hip (violating assumption 4.i). We attempted to compensate for this effect with a counterbalance visible in Fig. 2, but an unacceptably large weight would have been required to completely correct the problem.

In the video attachment, we include clips of the robot

hopping along a boom, with varying degrees of physical constraint corresponding to the “bodies” of Fig. 7 (annotated in the video). The controller implemented on the hardware is agnostic of the physical constraint, and takes the decoupled form of a cross-product of the rows of Table II.

VII. DISCUSSION AND CONCLUSION

Raibert’s hopper [13] made significant empirical advances in the field of robotics, but to our knowledge, no previous account in the literature has provided any formal conditions under which such simple and decoupled control strategies will work. In this paper, we apply simple decoupled controllers using similar ideas (including the exact same fore-aft (8) and pitch (16) controllers), but with a new vertical hopping scheme (§III-A) and a new tail appendage to enable it. Moreover, we construct abstract models (that appear to, nevertheless, be representative of empirical data) that enable us to present analyses of stability for each of these subsystems, and make steps towards a local proof of stability for the tailed hopper (a subject of future work by the authors).

The first focus of future work is a complete analysis of stability of tail-energized hopping on the Jerboa, and development of formal tools for design and verification of parallel composition. Second, our analysis in this paper is very specifically targetted to the tailed hopper (including the hand-designed hierarchy in Fig. 1), but in future work we plan to generalize these ideas to other tasks as well as platforms. As explained in §II, we focus on closed-loop templates in this paper, but there is an accompanying interesting problem of assignment of actuator affordances to the control of specific compartments. Lastly, we see in this paper that a sufficient condition for enabling a simple parallel composition is a physical decoupling (§V-B) through the design (summarized in assumption 4) and natural dynamics of the system. In the future we wish to leverage recent advances in self-manipulation [28] to enable a direct analysis of the system dynamics, perhaps even enabling tools for designing machines based on a desired composition hierarchy (Fig. 1).

REFERENCES

- [1] E. Westervelt and J. Grizzle, *Feedback Control of Dynamic Bipedal Robot Locomotion*, ser. Control and Automation Series. CRC Press/INC, 2007.
- [2] R. Tedrake, “Underactuated robotics: Learning, planning, and control for efficient and agile machines course notes for MIT 6.832,” Tech. Rep., 2009.
- [3] P. Holmes, R. J. Full, D. Koditschek, and J. Guckenheimer, “The dynamics of legged locomotion: Models, analyses, and challenges,” *Siam Review*, vol. 48, no. 2, pp. 207–304, 2006.
- [4] M. Buehler, D. Koditschek, and P. Kindlmann, *A simple juggling robot: Theory and experimentation*, ser. Lecture Notes in Control and Information Sciences, 1989, vol. 139, pp. 35–73.
- [5] L. L. Whitcomb, A. A. Rizzi, and D. E. Koditschek, “Comparative experiments with a new adaptive controller for robot arms,” *IEEE Trans. on Robotics and Automation*, vol. 9, no. 1, pp. 59–70, 1993.
- [6] S. A. Burden, S. Revzen, S. S. Sastry, and D. E. Koditschek, “Event-selected vector field discontinuities yield piecewise-differentiable flows,” *arXiv:1407.1775 [math]*, Jul 2014, arXiv: 1407.1775.
- [7] J. Nakanishi, T. Fukuda, and D. E. Koditschek, “A brachiating robot controller,” *IEEE Transactions on Robotics and Automation*, vol. 16, no. 2, pp. 109–123, 2000.
- [8] U. Saranlı, W. J. Schwind, and D. E. Koditschek, “Toward the control of a multi-jointed, monopod runner,” in *1998 IEEE International Conference on Robotics and Automation*, vol. 3, 1998, pp. 2676–2682.
- [9] R. J. Full and D. E. Koditschek, “Templates and anchors: neuromechanical hypotheses of legged locomotion on land,” *Journal of Exp. Biology*, vol. 202, no. 23, pp. 3325–3332, Dec. 1999.
- [10] R. Blickhan and R. J. Full, “Similarity in multilegged locomotion: Bouncing like a monopode,” *Journal of Comparative Physiology A: Sensory, Neural, and Behavioral Physiology*, vol. 173, no. 5, pp. 509–517, 1993.
- [11] T. Libby, T. Y. Moore, E. Chang-Siu, D. Li, D. J. Cohen, A. Jusufi, and R. J. Full, “Tail-assisted pitch control in lizards, robots and dinosaurs,” *Nature*, vol. 481, no. 7380, pp. 181–184, Jan. 2012.
- [12] A. M. Johnson, E. Chang-Siu, T. Libby, M. Tomizuka, R. J. Full, and D. E. Koditschek, “Tail assisted dynamic self righting,” in *Proc. Intl. Conf. on Climbing and Walking Robots*, 2012.
- [13] M. Raibert, *Legged Robots that Balance*, ser. Artificial Intelligence. MIT Press, 1986.
- [14] G. B. Gillis, L. A. Bonvini, and D. J. Irschick, “Losing stability: tail loss and jumping in the arboreal lizard *anolis carolinensis*,” *Journal of Experimental Biology*, vol. 212, no. 5, pp. 604–609, Mar. 2009.
- [15] T. E. Higham, M. S. Davenport, and B. C. Jayne, “Maneuvering in an arboreal habitat: the effects of turning angle on the locomotion of three sympatric ecomorphs of anolis lizards,” *Journal of Experimental Biology*, vol. 204, no. 23, pp. 4141–4155, Dec. 2001.
- [16] A. O. Pullin, N. J. Kohut, D. Zarrouk, and R. S. Fearing, “Dynamic turning of 13 cm robot comparing tail and differential drive,” in *Robotics and Automation (ICRA), 2012 IEEE International Conference on*. IEEE, 2012, pp. 5086–5093.
- [17] S. M. O’Connor, T. J. Dawson, R. Kram, and J. M. Donelan, “The kangaroo’s tail propels and powers pentapedal locomotion,” *Biology Letters*, vol. 10, no. 7, July 2014.
- [18] G. Sezer and U. Saranlı, “Control of monopedal running through tunable damping,” in *2013 21st Signal Processing and Communications Applications Conference (SIU)*, Apr. 2013, pp. 1–4.
- [19] O. Arslan and U. Saranlı, “Reactive planning and control of planar spring-mass running on rough terrain,” *IEEE Transactions on Robotics*, vol. 28, no. 3, pp. 567–579, June 2012.
- [20] A. De and D. E. Koditschek, “The Penn Jerboa: A platform for exploring parallel composition of templates,” Online: <http://arxiv.org/abs/1502.05347>, http://repository.upenn.edu/ese_reports/16, Tech. Rep., Feb 2015, arXiv:1502.05347.
- [21] S. Burden, S. Revzen, and S. S. Sastry, “Dimension reduction near periodic orbits of hybrid systems,” in *2011 50th IEEE Conference on Decision and Control and European Control Conference (CDC-ECC)*. IEEE, 2011, pp. 6116–6121.
- [22] D. E. Koditschek and M. Buehler, “Analysis of a simplified hopping robot,” *The International Journal of Robotics Research*, vol. 10, no. 6, pp. 587–605, Dec. 1991.
- [23] R. M. Ghigliazza, R. Altendorfer, P. Holmes, and D. Koditschek, “A simply stabilized running model,” *SIAM Review*, vol. 47, no. 3, pp. 519–549, Jan. 2005.
- [24] J. Pratt, J. Carff, S. Drakunov, and A. Goswami, “Capture point: A step toward humanoid push recovery,” in *2006 6th IEEE International Conference on Humanoid Robots*, 2006, pp. 200–207.
- [25] S. Kajita, F. Kanehiro, K. Kaneko, K. Fujiwara, K. Harada, K. Yokoi, and H. Hirukawa, “Biped walking pattern generation by using preview control of zero-moment point,” in *2003 IEEE International Conference on Robotics and Automation*, vol. 2, Sept. 2003, pp. 1620–1626 vol.2.
- [26] W. J. Schwind and D. E. Koditschek, “Control of forward velocity for a simplified planar hopping robot,” in *1995 IEEE International Conference on Robotics and Automation*, vol. 1, 1995, pp. 691–696.
- [27] H. Geyer, A. Seyfarth, and R. Blickhan, “Spring-mass running: simple approximate solution and application to gait stability,” *Journal of theoretical biology*, vol. 232, no. 3, pp. 315–328, 2005.
- [28] A. M. Johnson and D. E. Koditschek, “Legged self-manipulation,” *IEEE Access*, vol. 1, pp. 310–334, May 2013.
- [29] J. Schmitt and P. Holmes, “Mechanical models for insect locomotion: dynamics and stability in the horizontal plane i. theory,” *Biological cybernetics*, vol. 83, no. 6, pp. 501–515, Dec. 2000.
- [30] D. E. Koditschek, “Adaptive techniques for mechanical systems,” in *Proc. 5th. Yale Workshop on Adaptive Systems*, May 1987, pp. 259–265.
- [31] A. M. Johnson and D. E. Koditschek, “Toward a vocabulary of legged leaping,” in *Proc. ICRA 2013*, May 2013, pp. 2553–2560.